Published in final edited form as:
Curr Biol. 2007 November 20; 17(22): 1913–1924.

A novel requirement for *C. elegans* Alix/ALX-1 in RME-1 mediated membrane transport

Anbing Shi, **Saumya Pant**, **Zita Balklava**, **Carlos Chih-Hsiung Chen**, **Vanesa Figueroa**, and **Barth D. Grant**
Department of Molecular Biology and Biochemistry, Rutgers University, Piscataway, NJ 08854, USA

Summary

Background—Alix/Bro1p family proteins have recently been identified as important components of multivesicular endosomes (MVEs) involved in the sorting of endocytosed integral membrane proteins, interacting with components of the ESCRT complex, the unconventional phospholipid LBPA, and other known endocytosis regulators. During infection Alix can be co-opted by enveloped retroviruses, including HIV, providing an important function during virus budding from the plasma membrane. In addition Alix is associated with the actin cytoskeleton and may regulate cytoskeletal dynamics.

Results—Here we demonstrate a novel physical interaction between the only apparent Alix/Bro1p family protein in *C. elegans*, ALX-1, and a key regulator of receptor recycling from endosomes to the plasma membrane called RME-1. Analysis of *alx-1* mutants indicates that ALX-1 is required for endocytic recycling of specific basolateral cargo in the *C. elegans* intestine, a pathway previously defined by analysis of *rme-1* mutants. Expression of truncated human Alix in HeLa cells disrupts recycling of MHCI, a known Ehd1/RME-1 dependent transport step, suggesting phylogenetic conservation of this function. We show that the interaction of ALX-1 with RME-1 in *C. elegans*, mediated by RME-1/YPSL and ALX-1/NPF motifs, is required for this recycling process. In the *C. elegans* intestine ALX-1 localizes to both recycling endosomes and MVEs, but the ALX-1/RME-1 interaction appears dispensable for ALX-1 function in MVEs/late endosomes.

Conclusions—This work provides the first demonstration of a requirement for an Alix/Bro1p family member in the endocytic recycling pathway in association with the recycling regulator RME-1.

Introduction

The endocytic pathway of eukaryotes is essential for the internalization and trafficking of macromolecules, fluid, membranes, and membrane proteins. Membrane associated receptors and ligands are endocytosed either through clathrin-dependent or clathrin-independent uptake mechanisms [1,2]. After sorting in early endosomes, some cargo is transported from early to late endosomes and eventually to lysosomes for degradation [3]. Other cargo types recycle to the plasma membrane either directly, or indirectly via recycling endosomes [3,4]. Studies in HeLa cells indicate that receptors internalized via clathrin-dependent and clathrin-independent mechanisms meet in the endosomal system, but then recycle to the cell surface in distinct carriers [5].

Contact: Barth D Grant, 732-445-7340, Fax 732-445-4213, grant@biology.rutgers.edu.

In recent years it has become clear that Alix/Bro1p family proteins are conserved components of endosomal transport pathways. Alix and Bro1p are thought to function in the multivesicular endosome (MVE) pathway, promoting degradation of integral membrane proteins [6,7]. Multivesicular endosomes contain lumenal vesicles formed by inward invagination of the limiting membrane, and likely represent intermediates in the maturation of the pleiomorphic early/sorting endosomes into late endosomes [8]. Membrane proteins sorted into the lumenal vesicles of MVEs are degraded upon fusion of the MVEs with lysosomes in metazoans and with the vacuole in yeast [9]. The sorting of cargo, and budding of vesicles into the lumen of the MVE, depends on a network of proteins organized into four major hetero-oligomeric complexes and several monomeric or homo-oligomeric proteins: the Vps27/Hse1 complex (Hrs/STAM in humans), ESCRT-I, II, and III, the AAA ATPase Vps4, the ubiquitin hydrolase Doa4p, and Alix/Bro1p.

Alix and Bro1p contain a conserved ~380 amino acid “Bro1 domain” near their N termini [10,11]. Alix/Bro1p also contains a central V domain (aa 362-702 in Alix) consisting of two extended three-helix bundles and a conserved C-terminal Proline-Rich-Domain (PRD) [12]. The Bro1 domain is necessary for the endosomal localization of Alix/Bro1p and mediates membrane association through binding to the ESCRT-III complex subunit Snf7p/CHMP4b [6,13-15]. The PRD of Alix interacts with a number of endocytic regulatory proteins including SETA [16], endophilins [17], and the ESCRT-I complex subunit Tsg101 [18,19].

Through the second arm of its V domain, Alix also interacts with HIV-1 Gag and other retroviral proteins containing the motif YPXL, promoting the budding of viral particles from the plasma membrane [12,18-20]. Likewise the Aspergillus Alix homolog PalA interacts with the PacC protein through YPXL motifs [21]. *In vitro* Alix is preferentially recruited by liposomes containing the phospholipid 2,2′ lysobisphosphatidic acid (LBPA) [22]. LBPA is enriched in the internal membranes of MVEs and possesses the capacity to drive the formation of membrane invaginations within acidic liposomes [22]. It has been suggested that Alix is a target for this important lipid, potentially regulating the invagination process or back fusion of internal vesicles with the limiting membrane [22]. Alix also associates with structural proteins of the cytoskeleton, especially actin [23,24], and is important for the actin-dependent intracellular positioning of endosomes, and the formation of stress fibers, in tissue culture cells [23,25].

We and others have previously established *in vivo* endocytic assay systems for genetic analysis of trafficking in *C. elegans* tissues [26-29]. Among the endocytic regulators found in our screens we identified RME-1 [30]. *rme-1* mutants display endocytic recycling defects in several tissues [30], including strongly reduced uptake of yolk proteins by oocytes, due to poor recycling of yolk receptors, reduced uptake of fluid-phase markers by coelomocytes, and the accumulation of gigantic fluid-filled recycling endosomes in the intestinal cells, due to defective recycling of basolaterally endocytosed pseudocoelomic fluid. Evidence from studies of mammalian Ehd1/mRme-1 also indicates a function in recycling, specifically in the exit of membrane proteins from recycling endosomes [31]. All members of the RME-1 family contain a C-terminal EH domain [30,32]. The EH domain is associated with endocytic transport in mammalian cells and yeast [33,34]. Previous studies showed that the EH domain of RME-1 homologs, and other EH domain proteins, interact with target proteins through specific binding to sequences containing *Asparagine-Proline-Phenylalanine* (NPF) motifs [32,33,35]. In mammals, RME-1/Ehd1 forms protein complexes with Syndapin through EH-NPF interactions, which is important for recycling endosome function [36].

Here we show that *C. elegans* ALX-1 is physically associated with both recycling endosomes and MVEs, and provide evidence that ALX-1 functions with RME-1 in the *C. elegans* intestine, promoting the recycling of basolateral cargo internalized independently of clathrin. This

endocytic recycling regulation requires the RME-1/ALX-1 interaction, and is specifically mediated by RME-1-YPSL and ALX-1-NPF motifs.

Results

Physical association of ALX-1 and RME-1

In order to identify new regulators of endocytic recycling we performed a yeast two-hybrid screen for binding partners of RME-1, using the C-terminal region of RME-1 including the EH-domain (isoform D, amino acids 442-576) as bait. This screen identified several interacting clones encoding ALX-1, the *C. elegans* ortholog of human Alix/AIP1 and yeast Bro1p (Figure 1 and Materials and Methods). We confirmed the binding interaction using an *in vitro* GST-pulldown assay (Supplementary Figure S1, as indicated). The novel interaction that we detected between ALX-1 and the recycling endosome protein RME-1 suggested that ALX-1 might function on recycling endosomes, in addition to MVE's, or that RME-1 has a previously undetected function in the MVE.

To clarify interaction domains within RME-1 and ALX-1, we tested a series of truncated versions of the proteins in the two-hybrid assay. This analysis identified two modes of binding between the two proteins. First we noted that the extreme C-terminus of RME-1, just after the EH-domain, contains a tyrosine-proline-X-leucine (YPSL) motif, similar to that used by mammalian Alix to bind to retroviral Gag proteins [37], and that used by Aspergillus PalA to bind to PacC [21]. The central region of ALX-1 from amino acids 365-752 was sufficient to mediate the interaction, and deletion of the final nine amino acids of RME-1 including the YPSL sequence completely abrogated the interaction. In addition, we noted that the extreme C-terminus of ALX-1 contains an asparagine-proline-phenylalanine tri-peptide (NPF) motif. The EH-domain of RME-1 homologs, and other EH-domain proteins, are known to bind to NPF containing sequences [32,35]. Deletion of the NPF sequence in the context of the yeast two-hybrid prey construct reduced the RME-1/ALX-1 interaction by almost 3-fold, but did not completely block association (Figure 1). The Bro1 domain of ALX-1 was dispensable for the two-hybrid interaction. Taken together these results suggest that the central domain of ALX-1 contributes the main binding surface, interacting with the C-terminus of RME-1 through the YPSL containing tail, while the NPF sequence of ALX-1 interacts with the RME-1 EH-domain, perhaps modulating the interactions.

ALX-1 is broadly expressed in C. elegans

To determine what tissues express ALX-1, and are thus cell types where ALX-1 might interact with RME-1 *in vivo*, we created transgenic animals expressing a GFP-ALX-1 translational fusion gene driven by the *alx-1* promoter (see Materials and Methods). We observed ubiquitous expression of GFP-ALX-1 with notably high levels of expression in the intestine, hypodermis, body-wall muscles, nervous system, spermatheca, coelomocytes, and pharynx (Figure 2, A–F). The GFP-ALX-1 fusion protein appeared punctate in most tissues. In the intestine, GFP-ALX-1 was enriched near the apical PM and was also clearly enriched on distinct cytoplasmic puncta in the cytoplasm (Figure 2A, arrowheads). Intestine specific expression of equivalent fusions of ALX-1 to GFP or mCherry produced indistinguishable subcellular localization patterns and rescued *alx-1* mutant phenotypes (see below and Materials and Methods), indicating that the expression pattern and subcellular localization of the reporters very likely reflect those of the endogenous protein.

ALX-1 is associated with recycling endosomes and MVEs in the intestine

Since RME-1 and its mammalian homologs have not been found localized to MVEs, and are not required for membrane protein degradation, but rather are greatly enriched on recycling endosomes and function in recycling, we sought to determine if ALX-1 protein is present on

recycling endosomes. First we compared the subcellular localization of intestinally expressed mCherry-ALX-1 with GFP-RME-1, which is found on basolateral recycling endosomes [30, 38]. mCherry-ALX-1 colocalized extensively with GFP-RME-1 (Figure 3, A–C). Puncta positive for mCherry-ALX-1 and GFP-RME-1 were more frequent close to the basolateral PM and are best observed in the "Top" focal plane (Figure 3, A–C; Supplementary Figure S2, A-D). Fewer ALX-1 and RME-1 double-positive structures were found in the "Middle" focal planes that offer better views of the medial and apical membranes. These results indicated that ALX-1 is present on basolateral recycling endosomes where it could interact with RME-1 to regulate recycling. Our results also indicated that ALX-1 is present on other unidentified structures in the intestine. We obtained identical results with the fluorescent tags reversed, comparing GFP-ALX-1 with mCherry-RME-1.

Since mammalian Alix and yeast Bro1p are thought to be associated with MVEs, we also compared the localization of mCherry-ALX-1 with GFP-tagged HGRS-1 [39,40], the worm ortholog of the MVE protein Hrs/Vps27p. GFP-HGRS-1 mainly colocalized with mCherry-ALX-1 on puncta of the medial and apical cytoplasm (Figure 3, D–F, arrowheads; Supplementary Figure S2, E-H). These results suggest that ALX-1 is present on MVEs in addition to recycling endosomes. We confirmed that the RME-1-labeled recycling endosomes and the HGRS-1-labeled MVEs are independent vesicle populations by directly comparing the subcellular localization of GFP-HGRS-1 and mCherry-RME-1. We did not observe any colocalization between GFP-HGRS-1 and mCherry-RME-1 labeled puncta, substantiating this inference (Figure 3, G–I).

We also compared mCherry-ALX-1 with markers for early endosomes (GFP-RAB-5), late endosomes (GFP-RAB-7), and TGN/apical recycling endosomes (GFP-RAB-11) (Supplementary Figure S3). We observed occasional colocalization of mCherry-ALX-1 with the early endosome markers GFP-RAB-5 and did not observe colocalization with the TGN/ARE marker. mCherry-ALX-1 did not clearly label the large ring-like GFP-RAB-7 positive late endosomes, but some mCherry-ALX-1 puncta appeared on or near the rings. The weak colocalization with early and late endosome markers is consistent with the presence of ALX-1 on MVEs, since MVEs represent an intermediate in the maturation of early endosomes to late endosomes.

Taken together our results indicate that ALX-1 resides on two independent classes of endosomes in the worm intestine where it could potentially contribute to membrane traffic.

ALX-1 positive structure number increases in rme-1 mutants

As an additional test of the association of ALX-1 with recycling endosomes, we quantified the number of GFP-ALX-1 positive puncta in an *rme-1*(*b1045*) null mutant background. For comparison we also assayed GFP-HGRS-1, which is expected to label MVEs but not recycling endosomes. We previously established that *rme-1* mutant intestines specifically accumulate abnormally high numbers of basolateral recycling endosomes, but do not accumulate increased numbers of early, late, or apical recycling endosomes [38]. Thus if ALX-1 is associated with basolateral recycling endosomes we would expect to observe an increase in GFP-ALX-1 puncta number. *rme-1* null mutant intestines showed a nearly three-fold increase in GFP-ALX-1 puncta number, but no change in GFP-HGRS-1 puncta number (Figure 4, B and C; Supplementary Figure S4). These results are entirely consistent with residence of ALX-1 on basolateral recycling endosomes. These results also indicate that ALX-1 association with such endosomes does not require RME-1.

Loss of ALX-1 results in intracellular accumulation of recycling cargo

Given the physical association and colocalization of ALX-1 and RME-1, we sought to determine if loss of ALX-1 affects basolateral recycling. Toward this end we obtained a deletion allele of *alx-1*, *gk275*, created by the *C. elegans* Gene Knockout Consortium. This mutation deletes the first exon and part of the second exon, and is not predicted to produce any functional ALX-1 protein. *alx-1(gk275)* mutants are viable and at the gross organismal level appeared fairly normal, similar to *rme-1* mutants and several other endocytic trafficking mutants we have previously examined.

As a first step to determine if *alx-1* is required for basolateral recycling, we assayed the localization of basolaterally recycling transmembrane cargo proteins at steady-state, comparing wild-type animals with *alx-1*(*gk275*) mutant animals. Equivalent GFP-fusions for these cargo proteins have previously been shown to be functional and traffic normally in mammalian cells, and we have previously characterized them in the *C. elegans* intestine [38]. First we assayed for effects on the localization of the α-chain of the human IL-2 receptor TAC (hTAC-GFP), which is a marker for clathrin-independent uptake and *rme-1*-dependent recycling in mammalian cells [5,41], and which we have previously shown accumulates extensively in aberrant endosomes in *C. elegans rme-1* mutants [38]. We observed significant aberrant accumulation of hTAC-GFP in cytoplasmic puncta in *alx-1* mutant intestines. hTAC-GFP puncta number was increased by threefold in *alx-1* mutants compared with wild-type controls (Figure 5, C, D and E). These results suggest that the recycling of clathrin-independent cargo requires ALX-1.

We then assayed the human transferrin receptor (hTfR-GFP), which is a marker for clathrin-dependent uptake and *rme-1*-dependent recycling in mammalian cells [31,42,43]. We have previously shown that hTfR-GFP accumulates in aberrant endosomes in *C. elegans rme-1* mutants, but not as extensively as hTAC-GFP [38]. We could not detect any changes in localization for hTfR-GFP (Figure 5, A and B), suggesting that clathrin dependent cargo recycles normally in the absence of ALX-1.

In order to determine if human Alix is also required for recycling of clathrin-independent cargo, we analyzed major histocompatibility complex class I (MHCI) recycling in HeLa cells using a previously established pulse-chase assay that follows a non-perturbing anti-MHCI monoclonal antibody [44]. MHCI is a well documented marker for clathrin-independent uptake and Ehd1/mRme-1-dependent recycling in mammalian cells [41,45]. Cells transfected with an mRFP1 control vector were compared to cells co-transfected with mRFP1, and a FLAG-tagged dominant negative form of Alix (Alix-CT, amino acids 467-869) [46].

MHCI uptake was similar between mRFP1 transfected cells and mRFP1/FLAG-Alix(467-869) co-transfected cells (Figure 5, F, G and J). MHCI recycling in mRFP1/FLAG-Alix(467-869) co-transfected cells was reduced by 12-fold compared to control mRFP1 transfected cells (Figure 5, H, I and K), suggesting that the requirement for Alix/ALX-1 in this recycling pathway is conserved from worms to mammals.

We also analyzed clathrin-dependent cargo Tf uptake and recycling in HeLa cells using a previously described assay [47]. eGFP/FLAG-Alix(467-869) co-transfected cells showed slightly reduced, but not statistically different, Alexa568-Tf uptake (84.4%±9.8% of control, $p=0.055$), when compared to control cells transfected with EGFP control plasmid only. There was also no significant difference in the amount of recycled Alexa568-Tf between control eGFP transfected cells (62.2%±15.6%) and eGFP/FLAG-Alix(467-869) co-transfected cells (71.9%±13.9%), which is in agreement with previously published data using Alix siRNA [25].

alx-1 mutants accumulate abnormally high numbers of RME-1 positive endosomes

The increased number and size of hTAC-GFP labeled puncta in *alx-1* mutants suggested a block in hTAC recycling and a concomitant increase in basolateral recycling endosome number and size, similar to the phenotype of *rme-1* mutants [30,38]. To further analyze the effect of the *alx-1* knockout on recycling endosome number and size we quantified the number of GFP-RME-1 labeled endosomes in *alx-1* mutants. In wild-type animals, GFP-RME-1 strongly labels endosomes very near the basolateral PM (Figure 6A). GFP-RME-1 also weakly labels structures very near the apical PM that could be apical recycling endosomes [38]. In *alx-1* mutants an abnormally large number of GFP-RME-1 labeled endosomes accumulated, most notably appearing in large numbers throughout the cytoplasm in addition to the normally localized cortical structures (Fig 6B). Image quantitation revealed an approximately three-fold increase in GFP-RME-1 puncta number and size (Figure 6, I and J). No defects were found in the localization of an apical recycling endosome/TGN associated marker, GFP-RAB-11, in the intestine of *alx-1* mutants (Supplementary Figure S5). These results suggest that ALX-1 is important for the normal function of RME-1-positive basolateral recycling endosomes, and taken together with the effects on hTAC-GFP accumulation in worms, and MHCI recycling in HeLa cells, suggest that ALX-1/Alix is important for efficient export of certain cargo proteins from recycling endosomes. These results also indicate that ALX-1 is not required for the association of RME-1 with endosomes, suggesting that ALX-1 affects RME-1 function rather than its recruitment.

SDPN-1 recruitment to basolateral endosomes fails in alx-1 mutants

The F-Bar and SH3 domain protein Syndapin is a regulator of endocytic transport and actin dynamics. Previous work in HeLa cells showed that Syndapin is a binding partner of mammalian Ehd1/mRme-1 on recycling endosomes, and functions with Ehd1/mRme-1 in recycling [36]. This lead us to test if Syndapin is also involved in the basolateral recycling pathway described here. *C. elegans* has a single ortholog of syndapin, called SDPN-1, and we found that SDPN-1-GFP expressed from its own promoter is highly expressed in the intestine and colocalizes with RME-1 on basolateral recycling endosomes (data not shown). Further analysis showed that *alx-1* mutants lack SDPN-1 on basolateral structures, implying an inability to recruit SDPN-1 to basolateral endosomes (Figure 7, B and H). In *rme-1* mutants basolateral SDPN-1-GFP labeled structures were also significantly altered, characterized by loss of most basolateral SDPN-1-GFP labeled structures, and with many of the remaining structures appearing greatly enlarged (Figure 7, C and F). *alx-1* mutant animals depleted of RME-1 by RNAi displayed a mixed phenotype, with weaker SDPN-1-GFP labeling of endosomes that appeared enlarged, but less enlarged than in animals lacking RME-1 only (Figure 7, C and D). Apical SDPN-1 appeared normally localized in *alx-1* and *rme-1* mutants. Since Syndapin regulates membrane-associated actin dynamics and promotes membrane tubulation, failure to recruit SDPN-1 to basolateral recycling endosomes may be the primary defect resulting in intracellular accumulation of recycling cargo in *alx-1* mutants.

MVE and late endosome morphology is aberrant in alx-1 mutants

Analysis in early embryos indicated that ALX-1 is required for degradation of integral membrane proteins (see Supplemental results and Supplementary Figure S6, A-D), a process that does not require RME-1 but does require ESCRT proteins [48]. To assay for changes in the MVE/late endosome pathway in the intestine, we performed endosome morphometric analysis of *alx-1* mutant animals. We did not observe any effect of the loss of ALX-1 on RAB-5 positive early endosome number or size (Supplementary Figure S5). Consistent with a role for ALX-1 in intestinal MVE function we found a two-fold increase in MVE number and size in *alx-1* mutants in GFP-HGRS-1-expressing strains (Figure 6, D, I and J). We also observed a dramatic effect on GFP-RAB-7 and LMP-1-GFP positive late endosomes, which accumulated

in normal numbers but which displayed grossly abnormal morphology (Figure 6, F and H), with an average five-fold increase in late endosome size (Figure 6J). Consistent with our cargo analysis in *alx-1* mutant embryos, these results indicate that MVE and late endosome morphology, and likely their functions, require ALX-1 *in vivo*.

Basolateral recycling endosomes require the interaction of RME-1 with ALX-1

Finally, we sought to specifically test the role of the RME-1/ALX-1 interaction in transport, as opposed to the roles of the individual proteins. This was accomplished by reintroducing interaction defective forms of RME-1 or ALX-1 into their cognate null mutants and assaying for rescue of the loss-of-function phenotypes.

Our yeast two-hybrid studies indicated that RME-1 C-terminal tail containing the YPSL motif is required for RME-1 to bind to ALX-1. To determine the importance of the YPSL tail *in vivo*, and the contribution of ALX-1 binding to RME-1 function, we tested the ability of mCherry-RME-1 lacking the YPSL tail (mCherry-RME-1ΔYPSL) to rescue *rme-1(b1045)* mutants. Expression of mCherry-RME-1(+) or mCherry-RME-1(ΔYPSL) in *rme-1* null mutants fully rescued the formation of abnormal RE vacuoles containing accumulated basolaterally recycling fluid (Figure 7E), indicating that the interaction of RME-1 with ALX-1 is not required for fluid recycling. In stark contrast we found that expression of mCherry-RME-1(+), but not mCherry-RME-1(ΔYPSL), rescued the abnormal intracellular accumulation of hTAC-GFP and the abnormal localization/morphology of GFP-SDPN-1 (Figure 7F; Supplementary Figure S7). The failure of mCherry-RME-1(ΔYPSL) to rescue these phenotypes suggests that RME-1's function in SDPN-1 recruitment and hTAC recycling requires interaction with ALX-1.

In a similar set of experiments we compared the ability of mCherry-ALX-1 or mCherry-ALX-1 lacking the C-terminal NPF tri-peptide (mCherry-ALX-1ΔNPF) to rescue *alx-1* mutant phenotypes. Interestingly, we found that mCherry-ALX-1(ΔNPF) fully rescued *alx-1(gk275)* phenotypes associated with MVEs and late endosomes, including the abnormal increase in the number of GFP-HGRS-1-labeled endosomes and the size/morphology defects in LMP-1-GFP labeled late endosomes (Figure 7, G and H; Supplementary Figure S8). These results further confirm that RME-1 is not required for these functions of ALX-1. By contrast mCherry-ALX-1 (ΔNPF) could not rescue the recycling associated phenotypes of *alx-1* mutants, including hTAC-GFP accumulation or basolateral recruitment of GFP-SDPN-1 (Figure 7H; Supplementary Figure S8). As expected mCherry-ALX-1(+) rescued both the MVE/late endosome and RE associated phenotypes of *alx-1* mutants (Figure 7, G and H; Supplementary Figure S8). These results genetically separate the functions of ALX-1, indicating that the effects of *alx-1* mutants on hTAC and SDPN-1 are through RME-1 on recycling endosomes, and are not indirect effects produced by defective MVEs or late endosomes.

Discussion

In this study we show for the first time that an Alix/Bro1p family member functions in the endocytic recycling pathway, in association with the recycling endosome regulator RME-1. We also show that ALX-1 is required for the degradation of membrane proteins in *C. elegans*, likely functioning with the ESCRT machinery in the multivesicular endosome, as is thought to be the case for other members of the Alix/Bro1p family [7]. Consistent with our previous studies showing that RME-1 does not function in early or late endosomes, we found that RME-1 does not colocalize with HGRS-1-positive MVE's in the intestine and *rme-1* null mutants display normal degradation of membrane proteins in early embryos. In addition *rme-1* mutants display normal HGRS-1 labeled MVE morphology and number in the intestine. Thus our studies indicate a dual requirement for ALX-1 in both the recycling and degradative pathways, while RME-1 is specific for recycling.

Previous studies indicated that mammalian Alix facilitates virus budding from the plasma membrane of infected cells through direct binding to the sequence motif YPXL within viral Gag protein late-budding domains [18-20]. Similarly the Aspergillus Alix/Bro1p homologue PalA interacts with its partner protein PacC through YPXL motifs [21]. Our studies indicate an important interaction between the central region of ALX-1 and a C-terminal YPSL sequence in RME-1. In addition, the C-terminal NPF sequence in ALX-1 contributes to the interaction between ALX-1 and RME-1, presumably through the NPF-binding pocket present in the EH-domain. The NPF-mediated interaction between ALX-1 and RME-1 is required for the function of ALX-1 in recycling, but appears to be dispensable for ALX-1 function in MVE's/late endosomes. This genetic separation of the two functions of ALX-1 indicates mechanistic differences between ALX-1's roles in these two aspects of endocytic transport.

Consistent with a dual function for ALX-1 *in vivo*, we found evidence for ALX-1 localization to both types of endocytic organelles, the HGRS-1-positive MVE and the RME-1-positive recycling endosomes. Interestingly, recent studies in human T cells and macrophages using quantitative EM methods revealed an enrichment of endogenous human Alix on tubular-vesicular endosomal membranes containing transferrin, consistent with residence of human Alix on recycling endosomes [49]. Alix siRNA in HeLa cells was reported not to affect transferrin recycling but did affect endosome morphology [25]. In this study we found that expression of dominant negative Alix in HeLa cells dramatically interfered with MHCI recycling, but did not significantly affect transferrin recycling, suggesting that the role of Alix in recycling cargo endocytosed independently of clathrin is a conserved function. We note however that the interaction sites that we identified between *C. elegans* RME-1 and ALX-1 do not seem to be conserved in their human homologues. Similarly, although human Syndapin binds to Ehd1/mRme-1 directly, and worm SDPN-1 appears to function with RME-1 in recycling, the NPF containing sequences in Syndapin I and II recognized by Ehd1 are lacking in Ce-SDPN-1. Thus while our results suggest that these proteins function together in worms and mammals, the binding modes among those proteins may have been shuffled during metazoan evolution.

In yeast, the ALX-1 homolog Bro1p is required at the limiting membrane of specialized MVEs [7] for the sorting of mono-ubiquitinated membrane proteins into lumenal vesicles and productive transport to the vacuole [8]. However some controversy remains over the requirement for Alix in MVE-mediated degradation of membrane proteins, since Alix depleted HeLa cells were not delayed in the degradation of EGF receptors [25]. Alix is clearly required for the budding of retroviruses in mammals, another transport process that utilizes the MVE/ESCRT machinery [12,18-20]. In *C. elegans alx-1* mutants we observed defects in intestinal MVE/late endosome morphology and a very significant delay in the degradation of endocytosed membrane proteins CAV-1-GFP and RME-2-GFP in embryos, indicating conservation of this function in nematodes. Consistent with our results, Shaye and Greenwald [50] reported that degradation of LIN-12/Notch receptors in vulval precursor cells is delayed in animals depleted of ALX-1 by RNAi methods. Although there are no previously known mechanistic links between the degradative and recycling branches of the endocytic pathway, it may be advantageous for the cell to coordinate transport through multiple branches in the pathway, perhaps allowing a coordinated response to changes in cargo-type, overall cargo-load, and/or the local cellular environment.

While RME-1/mRme-1/Ehd1 is required for the efficient recycling of cargo internalized by clathrin-dependent and clathrin-independent mechanisms [30,31,38,41], our results suggest that ALX-1 is specifically required to recycle cargo of the clathrin-independent class. Consistent with this functional difference, not all basolateral RME-1 positive structures appear positive for ALX-1. Also, basolateral fluid recycling, that can likely utilize either RME-1 dependent recycling pathway, does not appear to require the RME-1/ALX-1 interaction.

While the mechanisms controlling the recycling of clathrin-independent cargo remain poorly defined, it is clear that local actin dynamics on endosomal membranes are important for productive transport of such cargo from recycling endosomes to the plasma membrane. For instance inhibition of actin polymerization using drugs such as latrunculin A or cytochalasin D, specifically disrupts recycling of clathrin-independent cargo in HeLa cells such as MHCI and Tac, while under the same conditions the clathrin-dependent cargo transferrin recycles normally [44,51,52]. Likewise the membrane associated actin regulator Arf6 is required to recycle clathrin-independent, but not clathrin-dependent cargos [5]. Interestingly knockdown of Alix in HeLa cells is known to perturb intracellular actin distribution, and Alix has been reported to copurify with cytoskeleton components, suggesting a possible functional link between Alix family proteins and membrane associated actin dynamics [23-25]. Syndapin is known to facilitate recruitment of N-WASP to membranes, thus activating Arp2/3-directed actin branching and polymerization [53,54]. We found that *alx-1* mutants showed greatly reduced recruitment of SDPN-1/Syndapin to basolateral endosomes, suggesting that ALX-1 promotes recycling through SDPN-1/Syndapin, and possibly N-WASP and the Arp2/3 machinery. As actin dynamics are thought to promote vesicle scission at the plasma membrane of yeast and mammalian cells, RME-1, ALX-1, and SDPN-1 may act in a similar way to promote endosomal carrier scission.

Supplementary Material

Refer to Web version on PubMed Central for supplementary material.

Acknowledgements

We thank J. Donaldson, R. Sadoul and C. Chatellard-Causse for important reagents. We also thank J. Donaldson, R. Weigert, C. Martin, P. Schweinsberg and Z. Pan for their generous advice and technical assistance. This work was supported by NIH Grant GM67237 to B.D.G.

References

1. Nichols B. Caveosomes and endocytosis of lipid rafts. Journal of cell science 2003;116:4707–4714. [PubMed: 14600257]
2. Gesbert F, Sauvonnet N, Dautry-Varsat A. Clathrin-lndependent endocytosis and signalling of interleukin 2 receptors IL-2R endocytosis and signalling. Current topics in microbiology and immunology 2004;286:119–148. [PubMed: 15645712]
3. Mukherjee S, Ghosh RN, Maxfield FR. Endocytosis. Physiological reviews 1997;77:759–803. [PubMed: 9234965]
4. Maxfield FR, McGraw TE. Endocytic recycling. Nature reviews 2004;5:121–132.
5. Naslavsky N, Weigert R, Donaldson JG. Characterization of a nonclathrin endocytic pathway: membrane cargo and lipid requirements. Molecular biology of the cell 2004;15:3542–3552. [PubMed: 15146059]
6. Katoh K, Shibata H, Suzuki H, Nara A, Ishidoh K, Kominami E, Yoshimori T, Maki M. The ALG-2-interacting protein Alix associates with CHMP4b, a human homologue of yeast Snf7 that is involved in multivesicular body sorting. The Journal of biological chemistry 2003;278:39104–39113. [PubMed: 12860994]
7. Odorizzi G, Katzmann DJ, Babst M, Audhya A, Emr SD. Bro1 is an endosome-associated protein that functions in the MVB pathway in Saccharomyces cerevisiae. Journal of cell science 2003;116:1893–1903. [PubMed: 12668726]
8. Katzmann DJ, Odorizzi G, Emr SD. Receptor downregulation and multivesicular-body sorting. Nature reviews 2002;3:893–905.
9. Gruenberg J, Stenmark H. The biogenesis of multivesicular endosomes. Nature reviews 2004;5:317–323.

10. Bateman A, Birney E, Cerruti L, Durbin R, Etwiller L, Eddy SR, Griffiths-Jones S, Howe KL, Marshall M, Sonnhammer EL. The Pfam protein families database. Nucleic acids research 2002;30:276–280. [PubMed: 11752314]
11. Kim J, Sitaraman S, Hierro A, Beach BM, Odorizzi G, Hurley JH. Structural basis for endosomal targeting by the Bro1 domain. Developmental cell 2005;8:937–947. [PubMed: 15935782]
12. Fisher RD, Chung HY, Zhai Q, Robinson H, Sundquist WI, Hill CP. Structural and Biochemical Studies of ALIX/AIP1 and Its Role in Retrovirus Budding. Cell 2007;128:841–852. [PubMed: 17350572]
13. Odorizzi G. The multiple personalities of Alix. Journal of cell science 2006;119:3025–3032. [PubMed: 16868030]
14. Katoh K, Shibata H, Hatta K, Maki M. CHMP4b is a major binding partner of the ALG-2-interacting protein Alix among the three CHMP4 isoforms. Archives of biochemistry and biophysics 2004;421:159–165. [PubMed: 14678797]
15. Gavin AC, Bosche M, Krause R, Grandi P, Marzioch M, Bauer A, Schultz J, Rick JM, Michon AM, Cruciat CM, et al. Functional organization of the yeast proteome by systematic analysis of protein complexes. Nature 2002;415:141–147. [PubMed: 11805826]
16. Schmidt MH, Hoeller D, Yu J, Furnari FB, Cavenee WK, Dikic I, Bogler O. Alix/AIP1 antagonizes epidermal growth factor receptor downregulation by the Cbl-SETA/CIN85 complex. Molecular and cellular biology 2004;24:8981–8993. [PubMed: 15456872]
17. Chatellard-Causse C, Blot B, Cristina N, Torch S, Missotten M, Sadoul R. Alix (ALG-2-interacting protein X), a protein involved in apoptosis, binds to endophilins and induces cytoplasmic vacuolization. The Journal of biological chemistry 2002;277:29108–29115. [PubMed: 12034747]
18. Strack B, Calistri A, Craig S, Popova E, Gottlinger HG. AIP1/ALIX is a binding partner for HIV-1 p6 and EIAV p9 functioning in virus budding. Cell 2003;114:689–699. [PubMed: 14505569]
19. von Schwedler UK, Stuchell M, Muller B, Ward DM, Chung HY, Morita E, Wang HE, Davis T, He GP, Cimbora DM, et al. The protein network of HIV budding. Cell 2003;114:701–713. [PubMed: 14505570]
20. Martin-Serrano J, Yarovoy A, Perez-Caballero D, Bieniasz PD. Divergent retroviral late-budding domains recruit vacuolar protein sorting factors by using alternative adaptor proteins. Proceedings of the National Academy of Sciences of the United States of America 2003;100:12414–12419. [PubMed: 14519844]
21. Vincent O, Rainbow L, Tilburn J, Arst HN Jr, Penalva MA. YPXL/I is a protein interaction motif recognized by aspergillus PalA and its human homologue, AIP1/Alix. Molecular and cellular biology 2003;23:1647–1655. [PubMed: 12588984]
22. Matsuo H, Chevallier J, Mayran N, Le Blanc I, Ferguson C, Faure J, Blanc NS, Matile S, Dubochet J, Sadoul R, et al. Role of LBPA and Alix in multivesicular liposome formation and endosome organization. Science 2004;303:531–534. [PubMed: 14739459]
23. Pan S, Wang R, Zhou X, He G, Koomen J, Kobayashi R, Sun L, Corvera J, Gallick GE, Kuang J. Involvement of the conserved adaptor protein Alix in actin cytoskeleton assembly. The Journal of biological chemistry 2006;281:34640–34650. [PubMed: 16966331]
24. Schmidt MH, Chen B, Randazzo LM, Bogler O. SETA/CIN85/Ruk and its binding partner AIP1 associate with diverse cytoskeletal elements, including FAKs, and modulate cell adhesion. Journal of cell science 2003;116:2845–2855. [PubMed: 12771190]
25. Cabezas A, Bache KG, Brech A, Stenmark H. Alix regulates cortical actin and the spatial distribution of endosomes. Journal of cell science 2005;118:2625–2635. [PubMed: 15914539]
26. Fares, H.; Grant, B. Traffic. 3. Copenhagen, Denmark: 2002. Deciphering endocytosis in Caenorhabditis elegans; p. 11-19.
27. Grant B, Hirsh D. Receptor-mediated endocytosis in the Caenorhabditis elegans oocyte. Molecular biology of the cell 1999;10:4311–4326. [PubMed: 10588660]
28. Sato, M.; Grant, BD. Intracellular trafficking. In: T.C.e.R. Community. , editor. WormBook. WormBook;
29. Fares H, Greenwald I. Genetic analysis of endocytosis in Caenorhabditis elegans: coelomocyte uptake defective mutants. Genetics 2001;159:133–145. [PubMed: 11560892]

30. Grant B, Zhang Y, Paupard MC, Lin SX, Hall DH, Hirsh D. Evidence that RME-1, a conserved C. elegans EH-domain protein, functions in endocytic recycling. Nature cell biology 2001;3:573–579.
31. Lin SX, Grant B, Hirsh D, Maxfield FR. Rme-1 regulates the distribution and function of the endocytic recycling compartment in mammalian cells. Nature cell biology 2001;3:567–572.
32. Naslavsky N, Caplan S. C-terminal EH-domain-containing proteins: consensus for a role in endocytic trafficking, EH? Journal of cell science 2005;118:4093–4101. [PubMed: 16155252]
33. Santolini E, Salcini AE, Kay BK, Yamabhai M, Di Fiore PP. The EH network. Experimental cell research 1999;253:186–209. [PubMed: 10579923]
34. Page LJ, Sowerby PJ, Lui WW, Robinson MS. Gamma-synergin: an EH domain-containing protein that interacts with gamma-adaptin. The Journal of cell biology 1999;146:993–1004. [PubMed: 10477754]
35. de Beer T, Hoofnagle AN, Enmon JL, Bowers RC, Yamabhai M, Kay BK, Overduin M. Molecular mechanism of NPF recognition by EH domains. Nature structural biology 2000;7:1018–1022.
36. Braun A, Pinyol R, Dahlhaus R, Koch D, Fonarev P, Grant BD, Kessels MM, Qualmann B. EHD proteins associate with syndapin I and II and such interactions play a crucial role in endosomal recycling. Molecular biology of the cell 2005;16:3642–3658. [PubMed: 15930129]
37. Puffer BA, Parent LJ, Wills JW, Montelaro RC. Equine infectious anemia virus utilizes a YXXL motif within the late assembly domain of the Gag p9 protein. Journal of virology 1997;71:6541–6546. [PubMed: 9261374]
38. Chen CC, Schweinsberg PJ, Vashist S, Mareiniss DP, Lambie EJ, Grant BD. RAB-10 is required for endocytic recycling in the Caenorhabditis elegans intestine. Molecular biology of the cell 2006;17:1286–1297. [PubMed: 16394106]
39. Roudier, N.; Lefebvre, C.; Legouis, R. Traffic. 6. Copenhagen, Denmark: 2005. CeVPS-27 is an endosomal protein required for the molting and the endocytic trafficking of the low-density lipoprotein receptor-related protein 1 in Caenorhabditis elegans; p. 695-705.
40. Yu X, Odera S, Chuang CH, Lu N, Zhou Z. C. elegans Dynamin mediates the signaling of phagocytic receptor CED-1 for the engulfment and degradation of apoptotic cells. Developmental cell 2006;10:743–757. [PubMed: 16740477]
41. Caplan S, Naslavsky N, Hartnell LM, Lodge R, Polishchuk RS, Donaldson JG, Bonifacino JS. A tubular EHD1-containing compartment involved in the recycling of major histocompatibility complex class I molecules to the plasma membrane. The EMBO journal 2002;21:2557–2567. [PubMed: 12032069]
42. Yamashiro DJ, Maxfield FR. Acidification of endocytic compartments and the intracellular pathways of ligands and receptors. Journal of cellular biochemistry 1984;26:231–246. [PubMed: 6085081]
43. Burack MA, Silverman MA, Banker G. The role of selective transport in neuronal protein sorting. Neuron 2000;26:465–472. [PubMed: 10839364]
44. Weigert R, Yeung AC, Li J, Donaldson JG. Rab22a regulates the recycling of membrane proteins internalized independently of clathrin. Molecular biology of the cell 2004;15:3758–3770. [PubMed: 15181155]
45. Naslavsky N, Weigert R, Donaldson JG. Convergence of non-clathrin-and clathrin-derived endosomes involves Arf6 inactivation and changes in phosphoinositides. Molecular biology of the cell 2003;14:417–431. [PubMed: 12589044]
46. Sadoul R. Do Alix and ALG-2 really control endosomes for better or for worse? Biology of the cell / under the auspices of the European Cell Biology Organization 2006;98:69–77. [PubMed: 16354163]
47. Weigert R, Donaldson JG. Fluorescent microscopy-based assays to study the role of Rab22a in clathrin-independent endocytosis. Methods in enzymology 2005;403:243–253. [PubMed: 16473591]
48. Audhya A, McLeod IX, Yates JR, Oegema K. MVB-12, a Fourth Subunit of Metazoan ESCRT-I, Functions in Receptor Downregulation. PLoS ONE 2007;2:e956. [PubMed: 17895996]
49. Welsch, S.; Habermann, A.; Jager, S.; Muller, B.; Krijnse-Locker, J.; Krausslich, HG. Traffic. 7. Copenhagen, Denmark: 2006. Ultrastructural Analysis of ESCRT Proteins Suggests a Role for Endosome-Associated Tubular-Vesicular Membranes in ESCRT Function; p. 1551-1566.
50. Shaye, DD.; Greenwald, I. Development. 132. Cambridge, England: 2005. LIN-12/Notch trafficking and regulation of DSL ligand activity during vulval induction in Caenorhabditis elegans; p. 5081-5092.

51. Brown FD, Rozelle AL, Yin HL, Balla T, Donaldson JG. Phosphatidylinositol 4,5-bisphosphate and Arf6-regulated membrane traffic. The Journal of cell biology 2001;154:1007–1017. [PubMed: 11535619]

52. Radhakrishna H, Donaldson JG. ADP-ribosylation factor 6 regulates a novel plasma membrane recycling pathway. The Journal of cell biology 1997;139:49–61. [PubMed: 9314528]

53. Qualmann B, Kelly RB. Syndapin isoforms participate in receptor-mediated endocytosis and actin organization. The Journal of cell biology 2000;148:1047–1062. [PubMed: 10704453]

54. Kessels MM, Qualmann B. The syndapin protein family: linking membrane trafficking with the cytoskeleton. Journal of cell science 2004;117:3077–3086. [PubMed: 15226389]

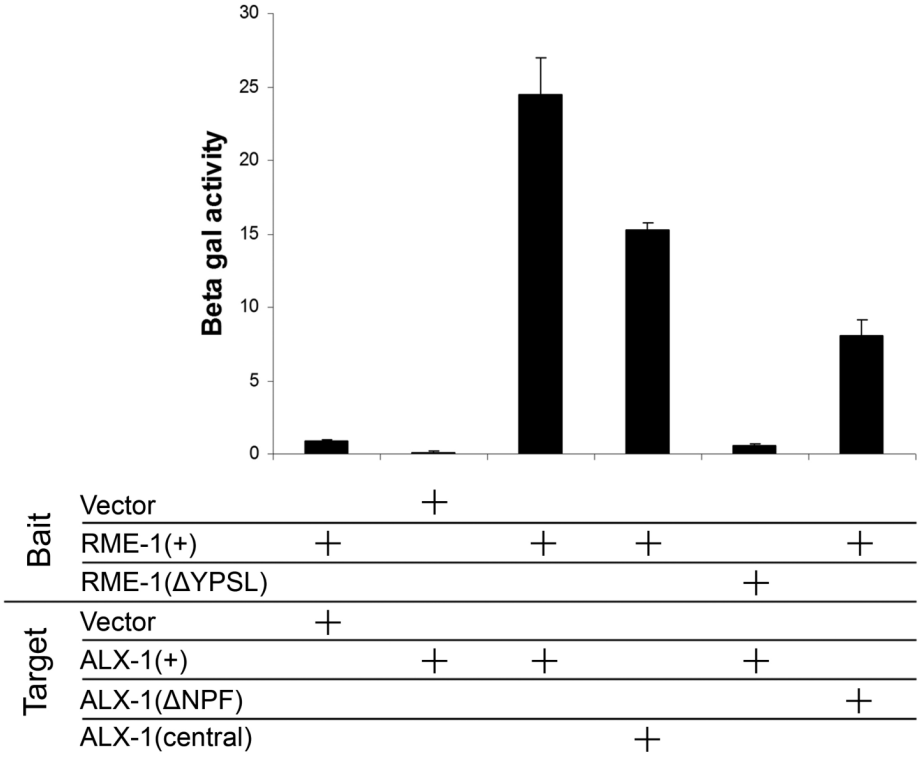

Figure 1. RME-1 Interacts with ALX-1

Quantitative yeast two-hybrid beta-galactosidase assays show that the ALX-1 C-terminal NPF motif contributes to the interaction with RME-1, while the central domain (aa 365-752) of ALX-1 contributes the main binding surface, interacting with RME-1 through its C-terminal YPSL sequence. Y-axis is labeled in Miller Units.

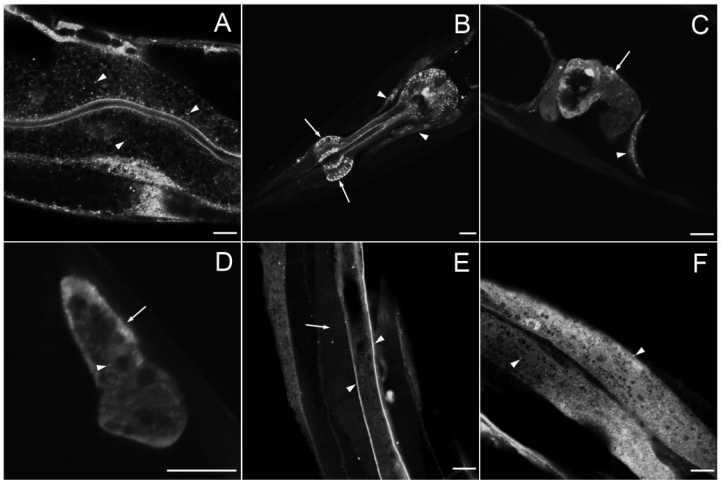

Figure 2. ALX-1 is Broadly Expressed in *C.elegans*

Expression of a GFP-ALX-1 transgene driven by the *alx-1* promoter is indicated in (A-F). (A) Intestine, arrowheads indicate cytoplasmic puncta. (B) Pharynx is indicated by arrows and nerve ring indicated by arrowheads. (C) Arrow indicates spermatheca and arrowhead indicates cytoplasmic puncta. (D) Coelomocyte, cytoplasmic puncta (arrowheads). (E) Nerve cord (arrowheads) and body-wall muscle (arrow). (F) Hypodermis, cytoplasmic puncta (arrowheads). Scale bars represent 10 μm.

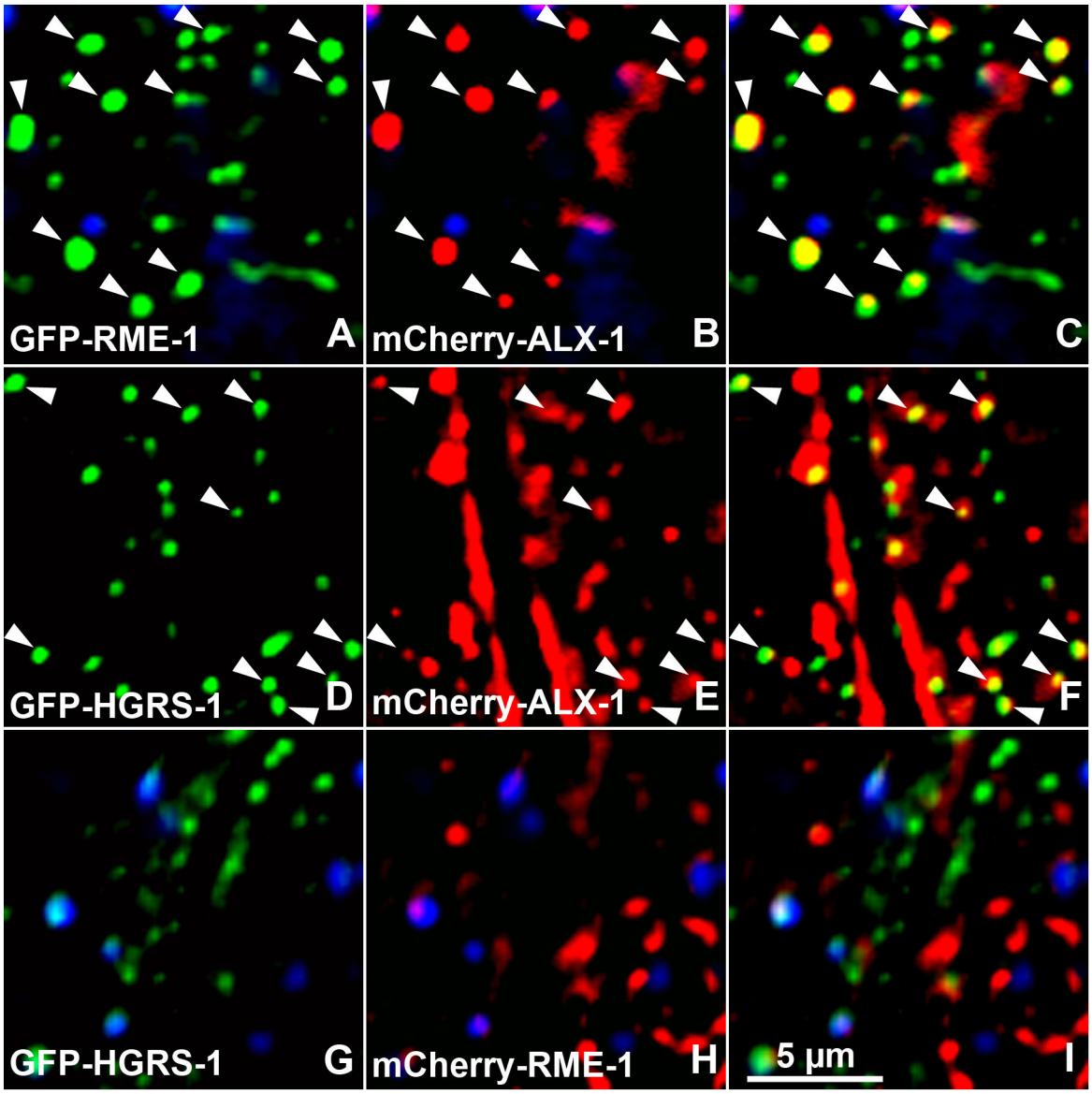

Figure 3. ALX-1 Associates with Two Types of Endosomes in the Intestine

(A-C) mCherry-ALX-1 colocalizes with GFP-RME-1 on basolateral recycling endosomes. Arrowheads indicate endosomes labeled by both GFP-RME-1 and mCherry-ALX-1. (D-F) Some mCherry-ALX-1 also colocalizes with MVE marker GFP-HGRS-1, mostly in the medial and apical cytoplasm. Arrowheads indicate puncta labeled by both mCherry-ALX-1 and GFP-HGRS-1. (G-I) mCherry-RME-1 and GFP-HGRS-1 label different endosome types. Virtually no overlap was observed between mCherry-RME-1 and GFP-HGRS-1. In each image autofluorescent lysosomes can be seen in all three channels with the strongest signal in blue, whereas GFP appears only in the green channel and mCherry only in the red channel. Signals observed in the green or red channels that do not overlap with signals in the blue channel are considered bone fide GFP or mCherry signals, respectively. Scale bar represents 5 μm.

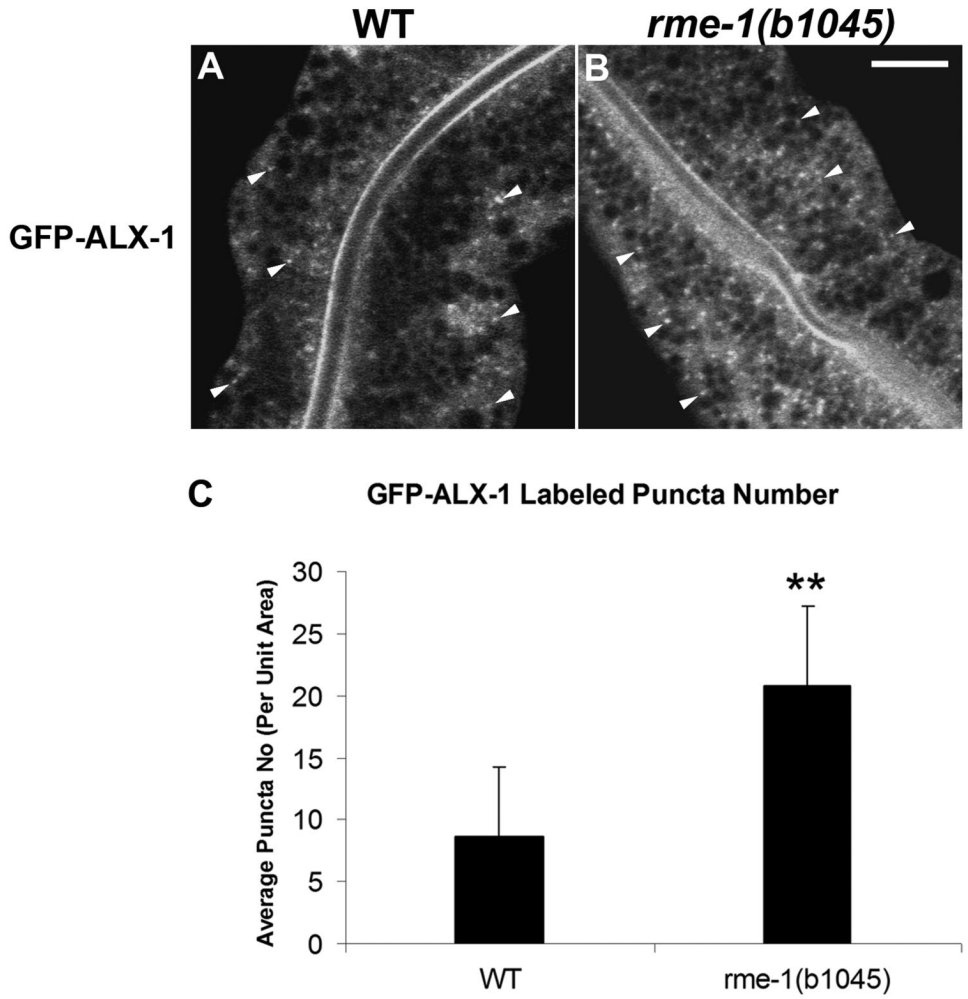

Figure 4. *rme-1* Mutants Accumulate Abnormally Numerous GFP-ALX-1 Labeled Endosomes

Confocal images of wild-type animals (A) and *rme-1(b1045)* mutant animals (B) showing GFP-ALX-1 labeled endosomes in the intestine. Arrowheads indicate GFP-ALX-1 puncta. (C) Quantification of endosome number in wild type animals and mutants as visualized by GFP-ALX-1. Error bars represent standard deviations from the mean (n=18 each, 6 animals of each genotype sampled in three different regions of each intestine). Asterisks indicate a significant difference in the one-tailed Student's t-test ($p<0.01$). Scale bar represents 10 μm.

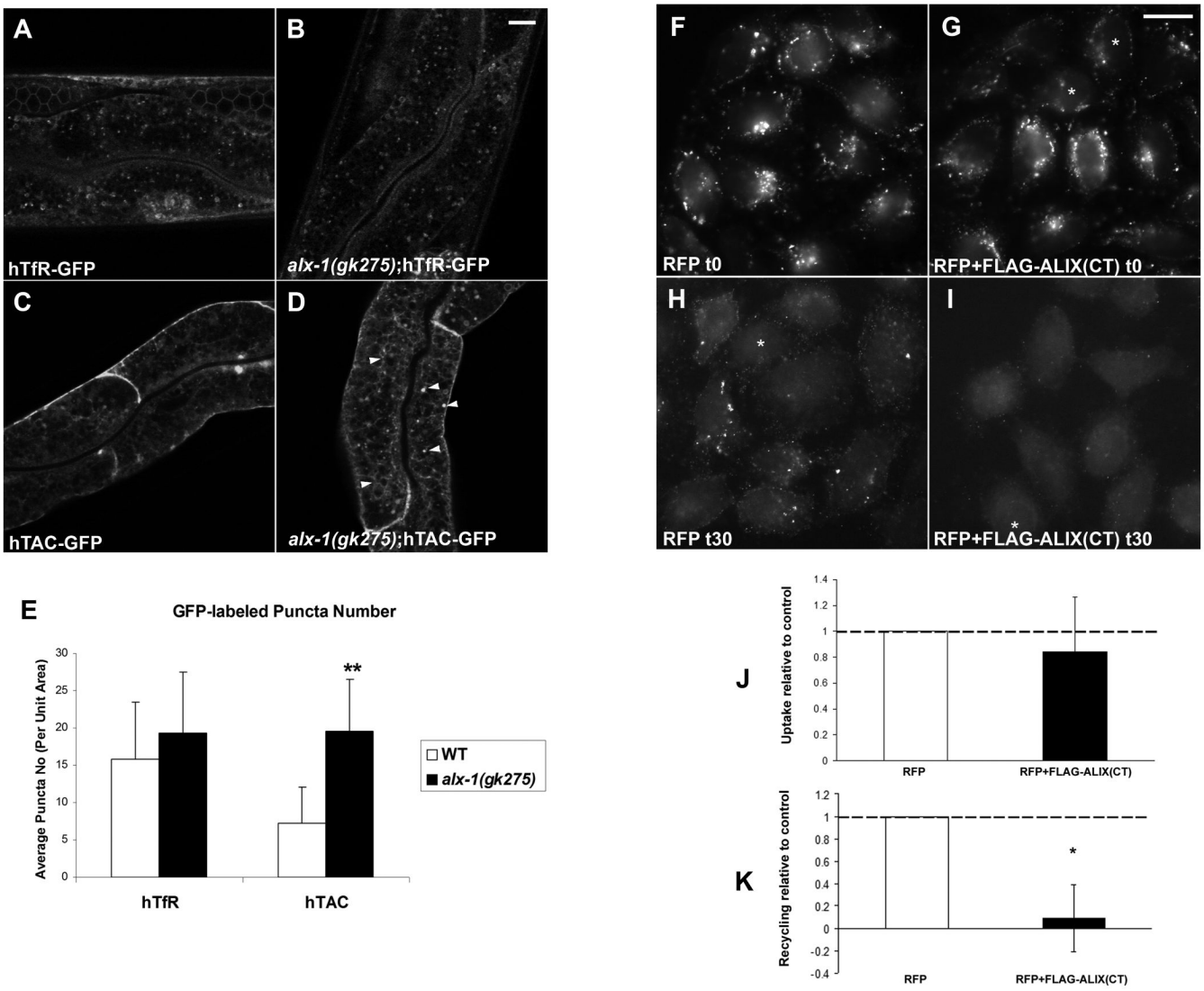

Figure 5. Abnormal Trafficking of Recycling Cargo in *alx-1* Mutant *C. elegans* and in HeLa Cells Expressing Truncated Alix

(A-B) Localization and morphology of hTfR-GFP, a clathrin-dependent cargo protein, appears unchanged in *alx-1(gk275)* mutants compared to wild-type animals. (C-D) hTAC-GFP, a cargo protein internalized independently of clathrin, becomes trapped in endosomal structures of *alx-1* mutants. Arrowheads indicate punctate and tubular endosomes labeled by hTAC-GFP in the intestine. (E) Quantification of cargo-labeled puncta number. Error bars represent standard deviations from the mean (n=18 each, 6 animals of each genotype sampled in three different regions of each intestine). (F-I) Representative images showing anti-MHCI labeling in control HeLa cells transfected with RFP expression plasmid only (F, H) or for cells co-transfected with RFP and truncated Alix expression plasmids (G, I). The first pair of images (F, G) show anti-MHCI uptake after 30 min incubation. The second pair of images (H, I) show surface MHCI after 30 minutes of recycling (H, I). Cells that were negative for the RFP signal are marked with asterisks. In co-transfection experiments these RFP-negative cells may or may not express Alix(467-869) (see Methods) and were therefore not included in the quantification. Conversely nearly all RFP expressing cells were found to also express FLAG-Alix(467-869) in control experiments. Therefore only RFP expressing cells were quantified for anti-MHCI uptake or

recycling. (J-K) The amount of MHCI antibody internalized after a 30 min pulse, or recycled after a 30 min chase, is shown as a ratio relative to control cells (see Methods). MHCI antibody recycling (K), but not MHCI antibody uptake (J), was impaired by expression of truncated FLAG-Alix(467-869). The asterisk in panel K indicates a significant difference in the one-tailed Student's t-test ($p=0.004$). Scale bars represent 10 μm in (A-D) and 20 μm in (F-I).

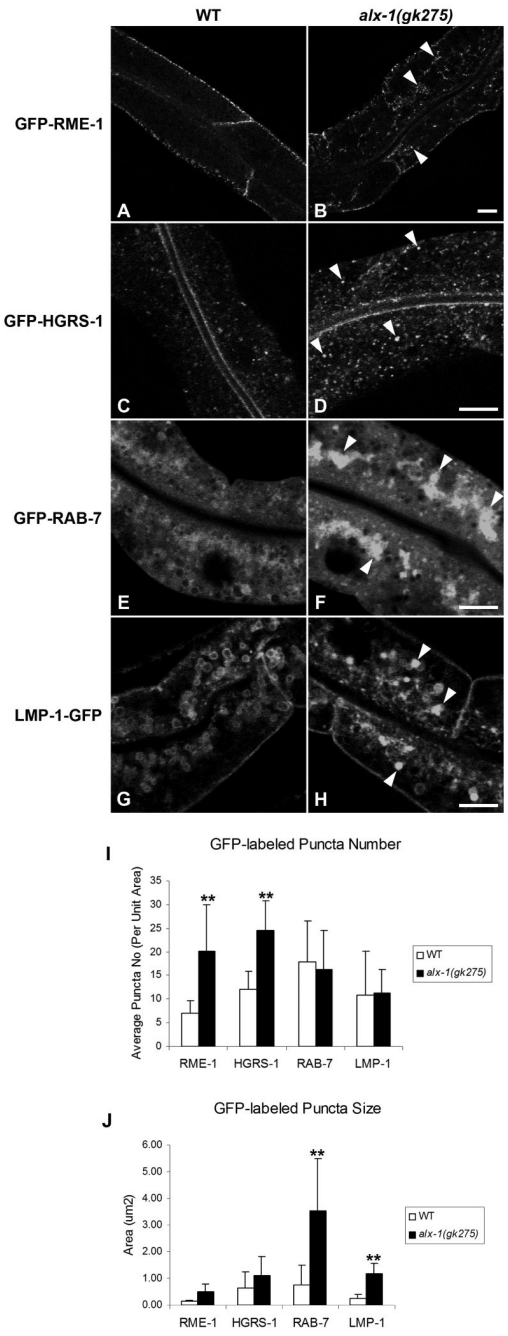

Figure 6. Altered Endosome Populations in *alx-1* Mutants

(A-B) GFP-RME-1 labeled recycling endosomes increase in number in *alx-1* mutant intestinal cells. Arrowheads indicate punctate and tubular endosomes labeled by GFP-RME-1. (C-D) GFP-HGRS-1 positive endosomes increase in number in *alx-1* mutant intestinal cells. Arrowheads indicate punctate endosomes labeled by GFP-HGRS-1. (E-H) GFP-RAB-7 and LMP-1-GFP labeled late endosomes appear enlarged and aggregated in *alx-1(gk275)* mutant intestinal cells. (J-K) Quantification of GFP-labeled puncta number and puncta size. Error bars represent standard deviations from the mean (n=18 each, 6 animals of each genotype sampled in three different regions of each intestine). The asterisks indicate a significant difference in the one-tailed Student's t-test ($p<0.01$). Scale bars represent 10 μm.

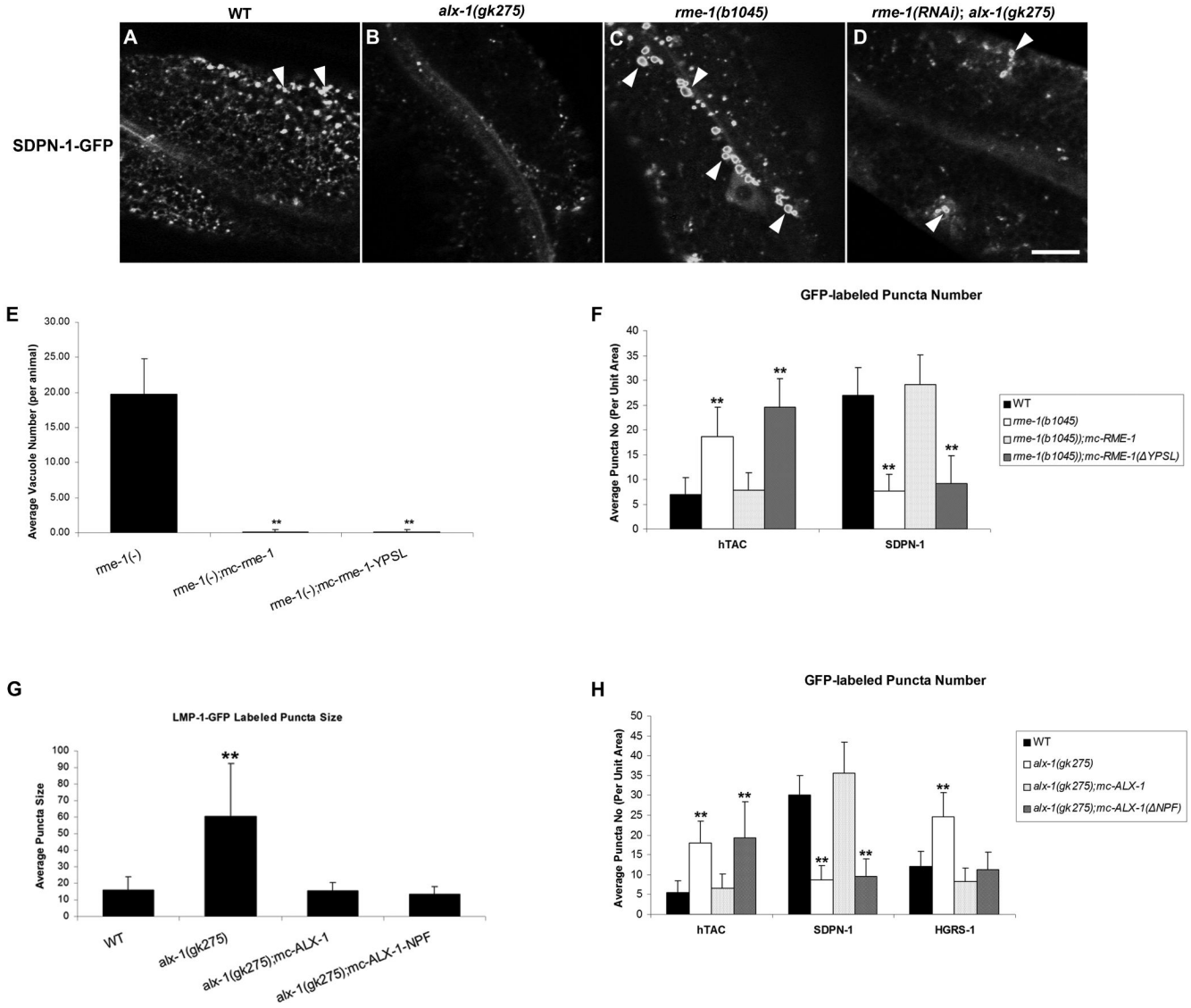

Figure 7. (A-D) Syndapin/SDPN-1-GFP Localization is Abnormal in *alx-1* Mutant and *rme-1* Mutant Intestinal Cells

(A) Confocal images of wild-type animals show abundant SDPN-1-GFP labeled basolateral punctate and tubular endosomes. (B) In *alx-1* mutant animals most basolateral SDPN-1-GFP positive structures are missing, and most of the remaining SDPN-1-GFP signal appears diffuse. (C) In *rme-1* mutant animals basolateral SDPN-1-GFP labeled structures are fewer, and many of those that remain are enlarged. (D) *alx-1(gk275); rme-1(RNAi)* animals lack most basolateral SDPN-1-GFP labeled structures like *alx-1* mutant animals, but the remaining structures appear enlarged. Arrowheads indicate endosomes labeled by SDPN-1-GFP. Scale bar represents 10 μm.

(E-H) Rescue Experiments Genetically Separate ALX-1 Functions and Indicate a Requirement for the ALX-1/RME-1 Interaction *in vivo*.

Interaction defective mutant forms of RME-1 (ΔYPSL) or ALX-1 (ΔNPF), expressed as mCherry (MC) fusions, were compared to wild-type forms in their ability to rescue specific *rme-1(b1045)* or *alx-1(gk275)* mutant phenotypes in the intestine. One set of phenotypes that were assayed focused on recycling endosomes: abnormal accumulation of basolaterally

recycling pseudocoelomic fluid in enlarged vacuoles/REs, intracellular recycling cargo hTAC-GFP accumulation, and basolateral SDPN-1-GFP recruitment/morphology. In addition, ALX-1(ΔNPF) was compared to intact ALX-1 in its ability to rescue *alx-1* mutant associated defects in the degradative pathway: multi-vesicular endosome number, as assayed by GFP-HGRS-1, and late endosome size, as assayed by LMP-1-GFP. (E) Expression of either MC-tagged RME-1 or MC-tagged RME-1(ΔYPSL) rescues basolateral fluid accumulation in *rme-1 (b1045)* mutants. (F) The last two bars in each group show the relative degree of rescue of *rme-1(b1045)* mutant defects achieved by expression of MC-tagged RME-1, or MC-tagged RME-1(ΔYPSL). Note that wild-type MC-RME-1 rescues both defects, while MC-RME-1 (ΔYPSL) cannot rescue the *rme-1(b1045)* associated defects. (G-H) The last two bars in each graph show the relative degree of rescue of *alx-1(gk275)* mutant defects achieved by expression of MC-tagged ALX-1, or MC-tagged ALX-1(ΔNPF). Note that wild-type MC-ALX-1 rescues all defects, while MC-ALX-1(ΔNPF) can only rescue *alx-1* associated phenotypes of the degradative pathway, LMP-1-GFP endosome size (G) and GFP-HGRS-1 puncta number (H), but cannot rescue phenotypes associated with the recycling pathway, hTAC-GFP and SDPN-1-GFP puncta number (H). Asterisks indicate a significant difference in the one-tailed Student's t-test ($p<0.01$).